Journal of Power Sources 191 (2009) 203–208

Contents lists available at ScienceDirect

Journal of Power Sources

journal homepage: www.elsevier.com/locate/jpowsour

Electrolyte effects on hydrogen evolution and solution resistance in microbial electrolysis cells

Matthew D. Merrill, Bruce E. Logan*

Department of Civil and Environmental Engineering, Pennsylvania State University, 212 Sackett Building, University Park, PA 16802, USA

ARTICLE INFO

Article history:
Received 12 January 2009
Received in revised form 19 February 2009
Accepted 20 February 2009
Available online 10 March 2009

Keywords:
Microbial electrolysis cell
Hydrogen evolution reaction
Weak acid catalysis
Electrolyte kinetics effects
Conductivity
Solution resistance

ABSTRACT

Protonated weak acids commonly used in microbial electrolysis cell (MEC) solutions can affect the hydrogen evolution reaction (HER) through weak acid catalysis, and by lowering solution resistance between the anode and the cathode. Weak acid catalysis of the HER with protonated phosphate, acetate, and carbonate electrolyte species improved MEC performance by lowering the cathode's overpotential by up to 0.30 V at pH 5, compared to sodium chloride electrolytes. Deprotonation of weak acids into charged species at higher pHs improved MEC performance primarily by increasing the electrolyte's conductivity and therefore decreasing the solution resistance between electrodes. The potential contributions from weak acid catalysis and solution resistance were compared to determine whether a reactor would operate more efficiently at lower pH because of the HER, or at higher pH because of solution resistance. Phosphate and acetate electrolytes allowed the MEC to operate more efficiently under more acidic conditions (pH 5). Carbonate electrolytes increased performance from pH 5 to 9 due to a relatively large increases in conductivity. These results demonstrate that specific buffers can substantially contribute to MEC performance through both reduction in cathode overpotential and solution resistance.

1. Introduction

A microbial electrolysis cell (MEC) is a promising new approach for producing hydrogen gas from biodegradable organic matter using exoelectrogenic microbes, but the rates of hydrogen production need to be improved [1,2]. The use of high surface area anodes, such as carbon fiber brush electrodes, provides a large surface area for microbes, and thus the reactor performance is usually not limited by the rate of oxidation of organic matter by the exoelectrogenic microbes [1,2]. Instead, the hydrogen evolution reaction (HER) on the cathode, and the solution resistance between electrodes, are primarily responsible for limitations in the MEC performance [1,2]. Microbes on the anode grow best under near-neutral pH conditions, and thus both electrodes in a membrane-less system are immersed in solutions at a pH near 7 that is maintained using a phosphate buffer [3], although carbonate buffers have been used in similar situations with microbial fuel cells [4]. The strength of the buffer affects the solution conductivity, and thus it has been well established that current densities can be increased through a decrease in solution resistance by increasing the concentration of the buffer or other electrolytes [5]. However, protonated weak acids in the solution can also substantially alter the efficiency of the MEC by directly affecting the overpotential for the HER. The relative effects of different electrolytes on the HER in concert with solution conductivity have not been systematically explored in prior MEC studies.

While strong acids or bases are used for water electrolyzers, it is also known that protonated weak acids can have a catalytic effect on hydrogen evolution [6]. Weak acids (HA) in greater activities than aqueous free protons (H^+) lower the hydrogen overpotential at lower current densities by donating protons to the HER through a weak acid catalytic effect [7–10]. It has been commonly reported that the rates of weak acid deprotonization and conjugate base re-protonization occur much faster than the rates of electron transfer [8–10,13,17–18] and so a pH gradient at the electrode surface due to the rates of proton consumption during catalysis would not be expected to occur. A limiting current density (J_l) is eventually reached where there is no increase in current despite the application of more negative potentials. The magnitude of the limiting current density has been correlated with the weak acid concentration [7–18], but prior work has focused almost exclusively on polished hemispherical Pt micro electrodes [7,8,10,11,13,14,17,18]. HER kinetics on larger electrodes are different than on polished hemispherical micro electrodes, where current densities can be ~10× larger and transport properties can have unusual effects, such as the suppression of bubble formation [7]. There has been little analysis on how the current changes with respect to overpotential below this limiting current density [9,16] (such as the Tafel slope), or on the potential at which the limiting current occurs. This analysis of HER at current densities below the limiting density is important for practical application of MECs as these systems will operate

* Corresponding author. Tel.: +1 814 863 7908; fax: +1 814 863 7304.
E-mail address: blogan@psu.edu (B.E. Logan).

0378-7753/$ – see front matter © 2009 Elsevier B.V. All rights reserved.
doi:10.1016/j.jpowsour.2009.02.077

at these lower current densities (1×10^{-4} to 1×10^{-3} A cm^{-2}), and thus we need a better understanding of how weak acids affect the HER for electrodes with large surface areas.

To better understand the effects of weak acids on MEC performance, phosphate, carbonate, acetate, and chloride electrolytes were selected here for analysis because of their relevance to MEC operation. Sodium phosphate is commonly used in the MEC medium because there is negligible metabolism of the electrolyte by the microbes, it is electrochemically stable, and it has a high conductivity per mole of anion [19–22]. Carbonate electrolytes are more likely to be the relevant electrolyte in natural waters and they have been shown in microbial fuel cells to optimize power generation at pH 9 [4]. Acetate is commonly used as a carbon source for the microbes in MECs [1,19–22] but it also functions as a monoprotic acid and thus its presence must also be included in this analysis. The concentration and ionization of these weak acids alters solution conductivity, and therefore experiments were also conducted using sodium chloride electrolytes. While a pH range of 5–9 is typically ideal for most exoelectrogenic microbes [3,4], a much larger pH range was examined in order to provide a better understanding of the electrolyte effects.

2. Methods

2.1. Electrochemical cell

The electrochemical cell (K0264 Micro-Cell, Princeton Applied Research, Oak Ridge) contained 15 ml sample of electrolyte solution that was sparged with ultrapure N_2 (GT&S, Inc., Allentown). The electrochemical cell consisted of vertical 1 cm^2 pure platinum (Hauser and Miller, St. Louis) working and counter electrodes, and a Ag/AgCl reference electrode placed in contact with the top edge of the working electrode. The platinum electrodes were pretreated using −0.5 to 2.0 V cyclic voltammetry scans at 200 mV s^{-1} until the peak hydrogen and oxygen evolution current densities became constant (∼5 cycles). The reference potential of the Ag/AgCl reference electrode was determined prior to each experiment with Zobell's solution and platinum electrodes [23]. Hydrogen evolution kinetics were measured with 1 mV s^{-1} linear voltammetry scans from +0.4 to ≤−1.4 V vs. NHE using the potentiostat's (PC4/750TM, Gamry, Warminster) ohmic drop compensation function. All experiments were performed in a constant temperature room (30 °C).

2.2. Analysis of solution chemistry

Visual MINTEQ version 2.53 (http://www.lwr.kth.se/English/OurSoftware/vminteq/) was used to predict electrolyte compositions so each solution in an electrolyte series was spaced ∼0.5 pH units apart. Electrolytes were prepared with ultrapure water (Milli-Q system, Billerica). Electrolyte solution conductivities per cm were measured with a conductivity probe and meter (Acorn Con6, Oakton, Vernon Hills), and solution pHs measured with a meter (Symphony SB21, Thermo Fisher Scientific, Waltham). The activities of the electrolyte species for the given conditions were calculated with MINTEQ using the measured pH values at 30 °C, and the following pK_a's were determined:

$$H_3PO_{4(aq)} \leftrightarrow H_2PO_4^{-}{}_{(aq)} + H^+ \quad (pK_a = 2.15) \tag{1}$$

$$H_2PO_4^{-}{}_{(aq)} \leftrightarrow HPO_4^{2-}{}_{(aq)} + H^+ \quad (pK_a = 7.20) \tag{2}$$

$$NaH_2PO_{4(aq)} \leftrightarrow NaHPO_4^{-}{}_{(aq)} + H^+ \quad (pK_a = 6.43) \tag{3}$$

$$HC_2H_3O_{2(aq)} \leftrightarrow C_2H_3O_2^{-}{}_{(aq)} + H^+ \quad (pK_a = 4.76) \tag{4}$$

$$HCO_3^{-}{}_{(aq)} \leftrightarrow CO_3^{2-}{}_{(aq)} + H^+ \quad (pK_a = 10.33) \tag{5}$$

$$NaHCO_{3(aq)} \leftrightarrow NaCO_3^{-}{}_{(aq)} + H^+ \quad (pK_a = 8.76) \tag{6}$$

2.3. HER kinetic analysis

Linear voltammetry scans were exported from the potentiostat's software (Echem Analyst, Gamry, Warminster) into Excel (Microsoft, Redmond). Logarithmic voltammograms were constructed where the reference potential of the Ag/AgCl electrode was subtracted from the measured potentials and plotted against the log of current density [24]. Tafel slopes were determined from the logarithmic voltammograms where the log of current density was linear with respect to potential and steepest at low overpotentials for a range of ≥30 mV. Hydrogen evolution is expected to be dependant upon pH by 0.0601 mV pH^{-1} at 30 °C [26] according to

$$E_0 = 0.000 - 2.303RTn^{-1}F^{-1}\ \log([H^+]^2[H_2]^{-1}) \tag{7}$$

Pourbaix diagrams represent electrochemical equilibria with pH on the *X*-axis and potential on the *Y*-axis [26]. The pH effects on the HER for a given electrolyte were illustrated three dimensionally with Matlab (Mathworks, Natick) by arranging a collection of logarithmic voltammograms according to Pourbaix diagrams wherein the log of current density was represented with color on the *Z*-axis.

2.4. Solution resistance

A theoretical analysis of the relationship between electrolyte conductivity and solution resistance is complicated by the reactor and electrode geometries. For example, dispersion in the field lines of ion conductance between the cathode and anode causes the geometry of the electrolyte volume between electrodes to affect the solution resistance in addition to just the distance between electrodes. The use of electrodes in MECs with complex geometries, such as brushes, further complicates this analysis. A simpler, more practical means of evaluating the relationship between electrolyte conductivity and the solution resistance in an MEC is to determine a cell constant, *K*, for the specific architecture for a given temperature, where *K* is related to solution conductivity, σ (S), by

$$\sigma = K \times R^{-1} \tag{8}$$

where *R* (Ω) is the solution resistance. *K* = 1 is equivalent to an ideal conductivity cell where 1 cm^2 square electrodes are spaced 1 cm apart in a cubic 1 cm^3 volume of electrolyte. The cell constant is determined by measuring the solution resistance using conductivity standards. Electrolyte solution resistance was determined by electrochemical impedance spectroscopy [24] with a potentiostat using calibration solutions (Traceable® One-Shot Conductivity Calibration Standards, Control Company, Friendswood) in the MEC reactor (no microorganisms). For the comparison of the electrolyte effects on the HER against the electrolyte's solution resistance, the total cell current of HER kinetics was measured in the MEC by linear sweep voltammetry (1 mV s^{-1}) using a potentiostat. The product of current and solution resistance was added to the potential at which the current was measured.

2.5. MEC reactor

The 4 cm cubic-shaped MEC reactor contains a cylindrical chamber 4 cm long × 3 cm in diameter, with the electrodes placed on each side of the chamber as previously described [19]. The cathode was platinized carbon cloth and the anode was a carbon fiber brush as described in more detail elsewhere [19].

3. Results

3.1. Logarithmic voltammogram analysis of electrolyte concentration effects

The presence of weak acid phosphate species lowered the HER overpotential by ∼0.3 V in 0.2 M $Na_XH_{(3-X)}PO_4$ at pH 6 (Fig. 1).

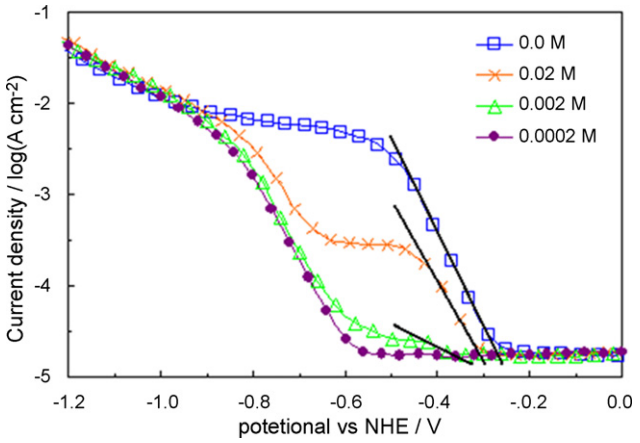

Fig. 1. HER logarithmic voltammograms for the weak acid catalytic effect in various concentrations of $Na_{1.185}H_{1.815}PO_4$ buffer in 0.2 M NaCl at pH 6. The solid lines indicate the kinetic region where the Tafel slope was derived.

Higher concentrations of phosphate electrolyte caused steeper Tafel slopes, indicating there was a greater increase in current density with overpotential. The limiting current densities changed by $\sim$1 log(A cm^{-2}) per log([phosphate electrolyte]) as expected from the literature [7–18]. HER kinetics were independent of the weak acid effects when the phosphate electrolyte was 0.0002 M or smaller. The inclusion of 0.2 M NaCl in the phosphate electrolytes prevented measurements from being limited by solution conductivity in tests with low phosphate concentrations. In addition, the potentiostat's ohmic drop compensation function was also used to prevent the electrolyte conductivity from affecting HER kinetics. The measurement of high current densities was prohibited for electrolytes with low conductivities when the total potential applied between the working and counter electrodes exceeded the potentiostat's maximum output of 4 V (Fig. 2).

3.2. Analysis of HER using NaCl

In contrast to the effect of the phosphate buffer on HER, the concentration of NaCl did not significantly affect the HER kinetics (Fig. 2). The pH dependence of the HER kinetics with respect to electrochemical potential is better visualized by combining all logarithmic voltammogram results in accordance with Pourbaix diagrams, with current density represented in color as the third dimension. HER kinetics in NaCl are seen to be independent of pH over the range of 3–12 because the kinetics did not change significantly in this range (see dashed line in Fig. 3). The lack of pH dependence for the HER kinetics between pH 3 and 12 suggests that water molecules were the reactant species for this case instead of H^+. The HER kinetics demonstrated pH dependence by changing -60 mV pH^{-1} (see solid line in Fig. 3). The limiting current densities decreased $\sim$1 log(A cm^{-2}) per log([H^+]) below pH 3, where H^+ was the reactant species. The lack of an effect of NaCl on the HER compared to the HER kinetic effects in buffered electrolytes, such as phosphate, provides direct evidence of the catalytic role of weak acids in addition to solution conductivity on MEC performance.

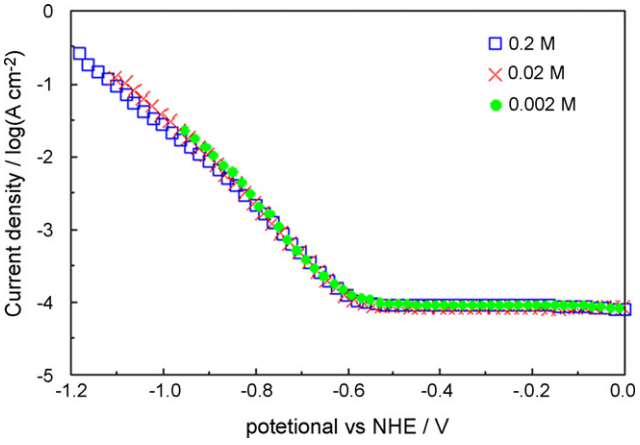

Fig. 2. Logarithmic voltammograms show that HER catalysis was independent of various concentrations of NaCl at pH 7.

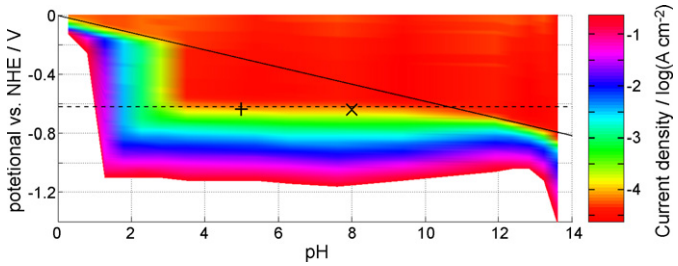

Fig. 3. The collection of HER logarithmic voltammograms for 0.2 M NaCl electrolytes with pH adjusted with HCl, NaOH, or a dilute phosphate solution (0.0002 M $Na_XH_{(3-X)}PO_4$). The solid line indicates a pH dependence of -60 mV pH^{-1} and the dashed line indicates a pH dependence of 0 mV pH^{-1}. Current densities of -4 log(A cm^{-2}) are indicated with + and $\times$ at pH 5 and 8, respectively.

3.3. Analysis of HER using phosphate

The HER kinetics were pH dependent at the lowest current densities in 0.2 M $Na_XH_{(3-X)}PO_4$ electrolytes (Fig. 4). This pH dependency is shown by a change of -60 mV pH^{-1} at current densities ≤ -4 log(A cm^{-2}). The low current density overpotentials were $\sim$0.35 to 0.15 V smaller in 0.2 M sodium phosphate electrolytes than in 0.2 M sodium chloride electrolytes between pH 5 and 8, respectively. At higher current densities the HER kinetics deviated from a pH dependence of 60 mV pH^{-1} at a given current density. The Tafel slope was at a maximum of 20.3 log(A cm^{-2}) V^{-1} at pH 6 and a minimum of 6.4 log(A cm^{-2}) V^{-1} at pH 8 (Supplemental Content, Fig. S1).

The limiting current densities were proportional to activities of protonated phosphate species except for the lowest pHs. The limiting current density observed from pH 2 to 4 correlated with the activity of H_3PO_4 [$\log(J_l) = 1.0 \times \log([H_3PO_4]) - 1.1$ log(A cm^{-2})] and from pH 5 to 7 the limiting current density correlated with the activity of $H_2PO_4^-$ by $\log(J_l) = 1.0 \times \log([H_2PO_4^-]) - 1.0$ log(A cm^{-2}) (Supplemental Content, Fig. S2). The linear relationship of J_l with $H_2PO_4^-$ failed at lower pH values (<pH 5) where the limiting current densities became disproportionately greater with respect to the phosphate species activities. Limiting current densities were not distinguishable at pH > 7 because the range of potentials in which weak acid kinetic effects were observed were too small for the cur-

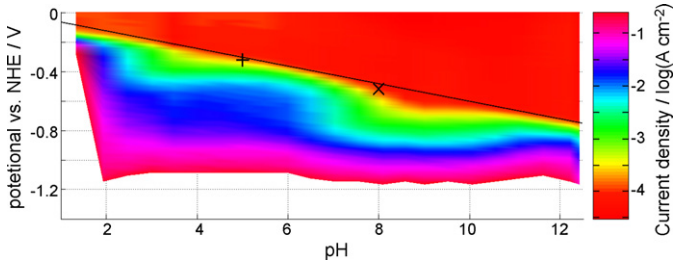

Fig. 4. The collection of HER logarithmic voltammograms for 0.2 M $Na_XH_{(3-X)}PO_4$ electrolytes. The solid line indicates a pH dependence of -60 mV pH^{-1}. Current densities of -4 log(A cm^{-2}) are indicated with + and $\times$ at pH 5 and 8, respectively.

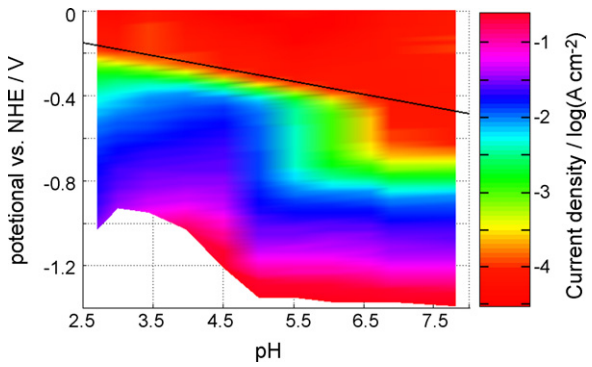

Fig. 5. The collection of HER logarithmic voltammograms for 0.2 M $Na_XH_{(1-X)}C_2H_3O_2$ electrolytes. The solid line indicates a pH dependence of −60 mV pH^{-1}.

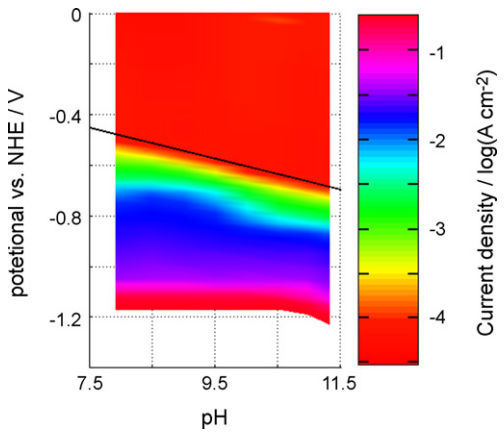

Fig. 6. The collection of HER logarithmic voltammograms for 0.2 M $Na_XH_{(2-X)}CO_3$ electrolytes. The solid line indicates a pH dependence of −60 mV pH^{-1}.

rent density to become completely limited with a $\Delta J\,\Delta V^{-1}$ of 0 (Supplemental Content, Fig. S1).

The most significant changes in HER kinetics were correlated with the pK_a's for phosphate at the relevant pH (Eq. (2) at pH 2.15; and Eqs. (3) and/or (4) at pH 7.20 and 6.43) as indicated by the change in colors near the pK_as (Fig. 4). The changes in activities of phosphate weak acids with respect to pH, in addition to the changes in Tafel slopes, resulted in HER kinetics that were primarily independent of pH at higher current densities.

3.4. Analysis of HER using acetate

The measurement of HER in sodium acetate electrolytes provided the clearest example of weak acid effects on the HER. The greatest changes in HER kinetics occurred near the pK_a = 4.76 of acetic acid (Eq. (4)) as shown by Fig. 5 where the Tafel slopes were steepest at $\sim$20 log(A cm^{-2}) V^{-1} in the pH region of 4–5.5. The current densities between −4 and −3.5 log(A cm^{-2}) were pH dependent at −60 mV pH^{-1} unit below pH 6.5. The HER kinetics in the sodium acetate electrolytes at pH 7 or higher were approximately the same (<4% log(A cm^{-2})) at a given potential as the sodium chloride electrolytes in the same pH range up to $\sim$−2.5 log(A cm^{-2}). The limiting current density observed from pH 5 to 7 correlated with the activity of $HC_2H_3O_2$, with $\log(J_l) = 1.0\log([HC_2H_3O_2]) - 1.0\log(A\,cm^{-2})$. However, the limiting current density was significantly lower than this below pH 4.5 (Supplemental Content, Fig. S3).

3.5. Analysis of HER using carbonate

The low current density HER kinetics were pH dependant at −60 mV pH^{-1} unit up to pH 11 (Fig. 6) for carbonate electrolytes. Similar to the phosphate electrolytes, the observed pH dependence resulted in hydrogen evolution overpotentials several tenths of a volt smaller in carbonate electrolytes than in sodium chloride electrolytes near neutral pH. Also similar to the phosphate electrolytes, limiting current densities were not distinguishable at the higher pH values because the range of potentials in which weak acid kinetic effects were observed were too small for $\Delta J\,\Delta V^{-1}$ to reach 0. A relationship between limiting current densities and electrolyte activities could therefore not be used to identify the electrolyte specie(s) responsible for the weak acid catalytic effect(s). The difference between carbonate and chloride kinetics, however, was likely caused by weak acid HER catalysis by the predominant electrolyte species H_2CO_3 and HCO_3^-. The activity of $NaHCO_3$ was only ≤10% that of HCO_3^-.

The analysis of HER in carbonate solutions was limited here to conditions greater than pH 8. HER kinetics below this pH could not be obtained as the pH changed faster than 0.01 pH $minute^{-1}$. This rapid change would have resulted in a pH change of >0.2 pH units during the LVS, and thus the pH would not have been sufficiently constant. The reason for the pH change was the thermodynamically favorable conversion of bicarbonate into insoluble carbon dioxide below pH 7.81 [18].

3.6. Effects of buffers on solution conductivity

The dissociation of weak acids into the charged conjugate base species at higher pHs increases the electrolyte's conductivity (Fig. 7) as measured with a conductivity meter. The greatest changes in electrolyte conductivity occurred near the pK_a(s). The increase in electrolyte conductivity decreases the solution resistance between the anode and cathode and therefore decreases the potential at which an MEC can sustain a given current density.

The relationship between electrolyte conductivity and the solution resistance was determined from an analysis of the cell constant using Eq. (1) in an MEC reactor. The cell constant K = 0.139 was unchanged for electrolyte conductivities <10 mS (Fig. 8 inset). Above 10 mS the relationship between electrolyte conductivity and solution resistance was not linear. This non-linear behavior was likely due to an increased amount of current reaching regions of the brush farther from the planar cathode at greater conductivities. Electrolytes with conductivities >10 mS therefore have an exponentially smaller solution resistance for this particular MEC architecture because of a greater utilization of the brush regions farther from the cathode.

The voltage reduction caused by weak acid HER catalysis at low pH was comparable in size to the voltage reduction caused

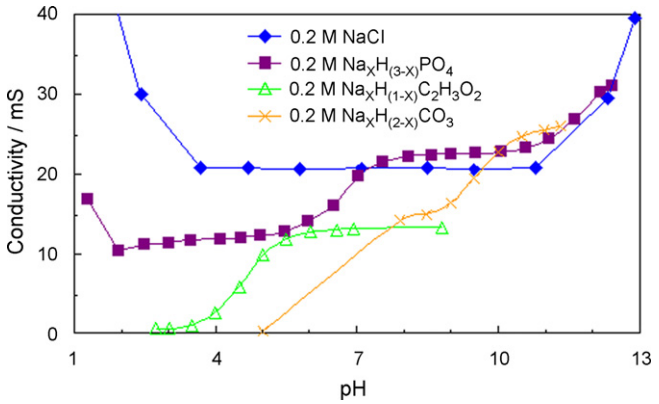

Fig. 7. Conductivities of the 0.2 M electrolyte solutions.

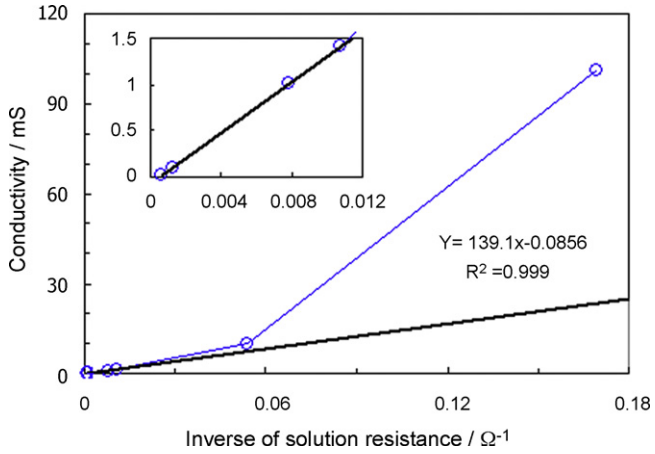

Fig. 8. The solution resistances of conductivity standards in a 4 cm cubic MEC reactor. Inset illustrates the linearity of low conductivity samples.

by lower solution resistances at higher pH for the MEC architecture. To determine whether cell performance would be better at lower pH because of weak acid HER catalysis or at higher pH because of conductivity, the voltage contributions from the solution resistance were factored into the logarithmic voltammogram's potential dependence by adding the product of current density and solution resistance to the working potential at which the current density was measured (Fig. 9). The current was greater at pH 5 for a given potential than at pH 8 when the total cell current was $\leq -1.85\ \log(\mathrm{A\,cm^{-2}})$ and the potential was ≤ -2.2 V. The sodium phosphate electrolytes at 0.2 M therefore performed better at lower pH because the potential effects of weak acid catalysis at pH 5 were greater than the potential effects of increased conductivity at pH 8.

Similar to the phosphate electrolytes, it would be more efficient in 0.2 M acetate electrolytes to operate at pH 5 than pH 8 for total cell currents $\leq$5 mA and potentials ≤ -1.4 V. The potential effects of weak acid catalysis may be smaller than the potential effects of conductivity for 0.2 M carbonate electrolytes because of the larger difference in conductivity between pH 5 and 8. A conductivity of only 0.3 mS was measured by sparging ultrapure water with CO_2 until pH 5. If the HER overpotential was -0.18 V ($-0.06\ \mathrm{V\ pH^{-1}} \times 3$ pH) smaller at low current densities in a pH 5 carbonate electrolyte compared to pH 8, this particular cell would operate more efficiently at pH 8 if the total cell current was greater than 0.4 mA. For a cell with a smaller constant (for example, a larger distance between electrodes), the cell would operate more efficiently at pH 8 for even lower total currents.

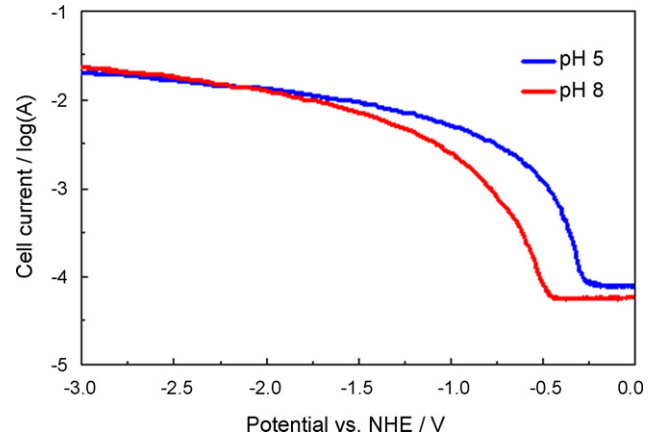

Fig. 9. Performance comparison for 0.2 M $Na_XH_{(3-X)}PO_4$ electrolytes in the 4 cm cubic MEC when the potential was applied to both the cathode and the electrolyte by adding the effects of solution resistance to the potential applied to the HER.

4. Discussion

The pH dependence of weak acid HER catalysis lowered the overpotential by several tenths of a volt at the lower current densities of -4.5 to $-2.5\ \log(\mathrm{A\,cm^{-2}})$ (Figs. 4–6) where MECs typically operate compared to the sodium chloride control (Fig. 3). This reduction in overpotential was not observed using only sodium chloride electrolytes at the same molar concentration (0.2 M) as can be seen by comparing Figs. 3 and 4. The lack of change in HER overpotential observed for various concentrations (0.2–0.0002 M) of sodium chloride electrolytes (Fig. 2) demonstrated that the HER catalytic effects were not dependant upon electrolyte conductivity. Only the solution resistance was dependant upon electrolyte conductivity.

The weak acid catalytic effect on the HER was dependant upon the weak acid's activity. The weak acid catalytic effect was not observed when the weak acid activity was <0.0002 M HA (Fig. 1). Lower HER overpotentials were observed for greater HA activities. The increase in current density would decrease with greater overpotentials and could become limited when $\Delta J\,\Delta V^{-1} = 0$. The current density could demonstrate limited behavior ($\Delta J\,\Delta V^{-1} \approx 0$) for a potential range of up to 0.15 V (Fig. 1). The limiting current density, J_l, was dependant upon HA activity as expected from the literature [5–15,25]. In general, there was a log–log relationship observed here between the J_l and the weak acid activity, or $\log(J_l) = 1.0\log([\mathrm{HA}]) - 1.0\log(\mathrm{A\,cm^{-2}})$. However, the relationship between J_l and the activity of $H_2PO_4^-$ has been previously reported in the literature to have discrepancies because the experimental J_l were small in comparison with their expected $H_2PO_4^-$ concentrations [14]. Visual MINTEQ accounts for the presence of NaH_2PO_4 in phosphate electrolytes, which has the effect of decreasing calculated $H_2PO_4^-$ activity. It was found here that the relationship between J_l and NaH_2PO_4 activity were similar to the relationships with H_3PO_4 and $HC_2H_3O_2$ activities and that Daniele et al.'s discrepancy [18] could be rectified by using Visual MINTEQ calculations for $H_2PO_4^-$ activities (Supplemental Content, Fig. S2). The presence of $NaHPO_4^-$ and NaH_2PO_4 and their effect on other phosphate species activities has been ignored in previous works on HER kinetics in phosphate electrolytes [5–8,14,15]. For example, the $NaHPO_4^-$ species was the predominant phosphate species between pH 7 and 11.5 (according to Visual MINTEQ), and because it has activities $\sim 2\times$ greater than HPO_4^{2-}, $NaHPO_4^-$ is likely the chemical species primarily responsible for the observed weak acid catalytic effects in this pH range. There were, however, substantial non-linear changes in the relationship between J_l and weak acid activity at lower pHs for both acetate and phosphate electrolytes. The J_l decreased disproportionately with respect to the concentration $HC_2H_3O_2$ below pH 4 (Supplemental Content, Fig. S3). The J_l increased disproportionately with respect to the concentration of H_3PO_4 at a pH 1.33 because of the contribution of bulk $[H^+]$ as reactants (Supplemental Content, Fig. S2). The J_l also increased disproportionately with respect to the concentration of $H_2PO_4^-$ below pH 5 (Supplemental Content, Fig. S2) and may have possibly been due to the reduction of phosphate species [19]. Together, the inability to include Tafel slope effects, the prior lack of factoring in all electrolyte species and activity coefficients, and unexplained deviations away from linear J_l vs. [weak acid] indicate that improvements in modeling weak acid catalysis of the HER are needed.

Weak acids affect MEC performance both with respect to the HER and the solution resistance. Protonated weak acids lower the cathode potential by facilitating HER catalysis while charged conjugate bases facilitate the conduction of ionic current between electrodes. Both of these effects are influenced by the cathode materials and

MEC architecture as well as the electrolyte. For example, limiting current densities and Tafel slopes have been reported to be different for Au [6] and Hg [9] than Pt. Also, a large variation (6.4–20.3 ($A\,cm^{-2}$)V^{-1}) in Tafel slopes with respect to pH for Pt in phosphate electrolytes were observed here, whereas Marinović et al. [15] reported a much smaller variation (6.2–6.7 log($A\,cm^{-2}$)V^{-1}) for Ag in the same electrolytes. The architecture of the cell, most importantly the distance(s) between electrodes, determines how much the electrolyte's conductivity affects the solution resistance. It is therefore important to understand whether a given MEC design will operate better at lower pH by capitalizing on weak acid catalysis of the HER or at higher pH because of lower solution resistances when the electrolyte conditions can be optimized. It is also important to understand how to distinguish whether a cell's performance is changing due to an alteration in the electrolyte composition (such as the consumption of acetate) or whether the cause is due to changes in the microbial community or because of catalyst degradation.

The greatest changes in both the weak acid HER catalytic effect and the electrolyte conductivity occur near the pK_a(s) of the predominant electrolyte species. The increases in weak acid activity below the pK_a mean that the majority of the weak acid HER catalytic effect is achieved 0.5–1.5 pH units below the pK_a. Similarly, the dissociation of weak acids into charged species means that the majority of the conductivity effect is achieved 0.5–1.5 pH units above the pK_a (Fig. 7). A given MEC weak acid electrolyte will therefore likely perform better at lower pH (5–6) by taking advantage of the hydrogen evolution catalysis or perform better at higher pH (8–9) by taking advantage of the conductivity effect. Phosphate electrolytes are likely to do better at lower pH because of relatively large conductivities at low pH (Fig. 9). Acetic acid and other monoprotic organic compounds with similar pK_as are also likely to do better at lower pH 5–6 because the HER catalytic effect (Fig. 5) would be combined with good conductivities (Fig. 7). For acetic acid at pH 8–9, the HER catalytic effect is lost (Fig. 5) while there is only a minimal increase in conductivity (Fig. 7). Carbonate electrolytes are, however, likely to do better at higher pH. The large pK_as of the carbonate electrolytes mean the HER catalytic effect occurs at high pHs (Fig. 6) where the electrolyte has large conductivities (Fig. 7). The large pK_as of carbonate also mean that the electrolyte has small conductivities at low pH (Fig. 7) because the majority of the carbonate species are protonated and therefore uncharged. More specific consideration of the effects of both the chemical species and the solution conductivity will lead to a better understanding of methods to optimize MEC performance.

Acknowledgements

We thank Shaoan Cheng for his insights into experimental setups. This research was funded by Air Products and Chemicals, Inc.

Appendix A. Supplementary data

Supplementary data associated with this article can be found, in the online version, at doi:10.1016/j.jpowsour.2009.02.077.

References

[1] B.E. Logan, D. Call, S. Cheng, H.V.M. Hamelers, T.H.J.A. Sleutels, A.W. Jeremaisse, R.A. Rozendal, Environ. Sci. Technol. 42 (23) (2008) 8630–8640.
[2] R.A. Rozendal, H.V.M. Hamlers, K. Rabaey, J. Keller, C.J.N. Buisman, Trends Biotechnol. 26 (2008) 450–459.
[3] Z. He, Y. Huang, A.K. Manohar, F. Mansfield, Bioelectrochemistry 74 (2008) 78–82.
[4] Y. Fan, H. Hu, H. Liu, Environ. Sci. Technol. 41 (23) (2007) 8154–8158.
[5] P. Atkins de Paula, J. Physical Chemistry, 7th ed., W.H. Freeman and Company, New York, 2002, pp. 833–834.
[6] Ya.V. Durdin, Uch. Zap. Leningr. Gos. Univ. im. A. A. Zhdanova. Ser. Khim. Nauk. 40 (1939) 3–18.
[7] M. Ciszkowska, Z. Stojek, S.E. Morris, J.G. Osteryoung, Anal. Chem. 64 (1992) 2372–2377.
[8] S. Daniele, I. Lavagnini, M.A. Baldo, F. Magno, J. Electroanal. Chem. 404 (1996) 105–111.
[9] V. Marinović, A. Despić, J. Serb. Chem. Soc. 63 (7) (1998) 545–553.
[10] C. Canhoto, M. Matos, A. Rodrigues, M.D. Geraldo, M.F. Bento, J. Electroanal. Chem. 570 (2004) 63–67.
[11] Z. Stojek, M. Ciszkowska, J.G. Osteryoung, Anal. Chem. 66 (1994) 1507–1512.
[12] M. Ciszkowska, Z. Stojek, J.G. Osteryoung, J. Electroanal. Chem. 398 (1995) 49–56.
[13] S. Daniele, M.A. Baldo, F. Simonetto, Anal. Chim. Acta 331 (1996) 117–123.
[14] M. Ciszkowska, A. Jaworski, J.G. Osteryoung, J. Electroanal. Chem. 423 (1997) 95–101.
[15] V. Marinović, A.R. Despić, J. Electroanal. Chem. 431 (1997) 127–132.
[16] V. Marinović, A.R. Despić, Russ. J. Electrochem. 33 (9) (1997) 965–970.
[17] S. Daniele, M.A. Baldo, C. Bragato, I. Lavagnini, Anal. Chim. Acta 361 (1998) 141–150.
[18] S. Daniele, I. Lavagnini, M.A. Baldo, F. Magno, Anal. Chem. 70 (2) (1998) 285–295.
[19] D. Call, B.E. Logan, Environ. Sci. Technol. 42 (2008) 3401–3406.
[20] S. Cheng, B.E. Logan, Proc. Natl. Acad. Sci. U.S.A. 104 (2007) 18871–18873.
[21] R. Rozendal, H.V.M. Hamlers, R.J. Molenkamp, C.J.N. Buisman, Water Res. 41 (2007) 1984–1994.
[22] H. Hu, Y. Fan, H. Lui, Water Res. 42 (2008) 4172–4178.
[23] D.K. Nordstron, F.D. Wilde, Techniques of Water-Resources Investigations Book 9, Chapter A6, United States Geological Survey. http://pubs.usgs.gov/twri/.
[24] A.J. Bard, L.R. Faulkner, Electrochemical Methods: Fundamentals and Application, 2nd ed., John Wiley & Sons, Hoboken, 2001.
[25] M. Pourbaix, Atlas of Electrochemical Equilibria in Aqueous Solution, Cebelcor, Brussels, 1974.